J. Pharm. Pharmacol. 1995, 47: 382–387
Received June 13, 1994
Accepted January 12, 1995

PEG-coated Poly(lactic acid) Nanoparticles for the Delivery of Hexadecafluoro Zinc Phthalocyanine to EMT-6 Mouse Mammary Tumours

ERIC ALLÉMANN, NICOLE BRASSEUR, OUHIDA BENREZZAK, JACQUES ROUSSEAU, SVETLANA V. KUDREVICH, ROSS W. BOYLE, JEAN-CHRISTOPHE LEROUX*, ROBERT GURNY* AND JOHAN E. VAN LIER

*MRC Group in the Radiation Sciences, Faculty of Medicine, University of Sherbrooke, Sherbrooke, Québec, Canada J1H 5N4, and *School of Pharmacy, University of Geneva, Switzerland*

Abstract

Hexadecafluoro zinc phthalocyanine ($ZnPcF_{16}$), a second generation sensitizer for the photodynamic therapy of cancer, was incorporated in three vehicles: poly(D,L-lactic acid) (PLA) nanoparticles, polyethylene glycol (PEG)-coated nanoparticles and a Cremophor EL (CRM) oil-water emulsion. Nanoparticles were prepared by the salting-out procedure. Biodistribution of the dye was assessed by fluorescence in EMT-6 mammary tumour bearing mice after intravenous injection of 1 μmol kg^{-1} $ZnPcF_{16}$.

Plain nanoparticles were rapidly retained by the reticuloendothelial system (RES) as reflected by the low area under the blood concentration–time curve (AUC_{0-168}, 57 $\mu g\ h\ g^{-1}$). Little tumour uptake of the dye was observed with this formulation. In contrast, PEG-coated nanoparticles displayed a reduced RES uptake, leading to significantly higher blood levels over an extended period ($t_{\frac{1}{2}}$ 30 h; AUC_{0-168} 227 $\mu g\ h\ g^{-1}$) and enhanced tumour uptake. At 48 h post injection, tumour to skin and tumour to muscle concentration ratios reached 3·5 and 10·8, respectively.

Blood levels of $ZnPcF_{16}$ after administration as a CRM emulsion decreased faster than with PEG-coated nanoparticles ($t_{\frac{1}{2}}$ 12 h), but since no early liver uptake was observed, the AUC_{0-168} and the tumour uptake were only slightly lower. However, with the CRM formulation, a late liver uptake was observed, reaching 51% of the injected dose after 7 days.

Photodynamic therapy of a variety of cancers with red light after systemic administration of a mixture of haematoporphyrin derivatives (Photofrin II) has now been approved in a number of countries to complement established treatment protocols such as surgery, radiotherapy and chemotherapy (Henderson et al 1994). Second generation photosensitizers of known composition and increased photodynamic activities are being developed to provide an alternative to Photofrin II. Phthalocyanines are promising agents for photodynamic therapy (van Lier 1990; Rosenthal 1991), primarily because of their advantageous photophysical properties, including a high molar absorption in the red region of the visible spectrum, where tissue transmission is optimal (Henderson & Dougherty 1992). Their photodynamic activities in-vivo largely depend on their pharmacokinetics and intratissular distribution. To improve the efficiency of photodynamic therapy there is a need to target the photosensitizer more accurately to malignant tissues. One way to satisfy this is to use colloidal drug delivery, such as nanoparticles (Brasseur et al 1991; Labib et al 1991) or liposomes (Jori et al 1983; Ginevra et al 1990).

Nanoparticles have received considerable attention as possible vehicles for drug targeting. However, unmodified nanoparticles suffer a major drawback in that they are massively taken up by the cells of the reticuloendothelial system (RES), mainly in the liver Kupffer cells and spleen macrophages. Consequently, nanoparticle uptake by other cells (e.g. tumour cells) remains quite low (Allémann et al 1993a). To circumvent this problem, investigators have focused on ways of modifying nanoparticle surface characteristics with the hope of altering the recognition by the RES. In-vivo studies with non-biodegradable nanoparticles have revealed the efficiency of poloxamers and poloxamines as efficient coatings to reduce liver sequestration (Illum & Davis 1987; Illum et al 1987; Tröster et al 1990; Tröster & Kreuter 1992; Tan et al 1993). Similar results were obtained with polyethylene glycol (PEG) when the latter was covalently bound to polystyrene nanoparticles (Dunn et al 1992). The importance of nanoparticle hydrophilicity and coating thickness in modifying the adsorption of plasma opsonins onto the surface of nanoparticles has been demonstrated. A recent study has shown that the uptake of poly(D,L-lactic acid) (PLA) nanoparticles by isolated human monocytes can be reduced significantly upon coating of the nanoparticles with PEG 20000 during the preparation procedure (Leroux et al 1994).

Based on these recent findings, the objective of this study was to compare the biodistribution of a phthalocyanine incorporated in three different formulations in EMT 6 mammary tumour-bearing mice: an oil/water emulsion of Cremophor EL (CRM), PLA nanoparticles and polyethylene glycol-coated PLA nanoparticles (PEG-coated nanoparticles). The nanoparticles were prepared by the salting-out procedure as described previously (Allémann et al 1992). CRM, a non-ionic polyoxyethylated castor oil surfactant of complex composition, has previously been used to solubilize hydrophobic photosensitizers for intravenous administration and appears to promote their tumour uptake (Selman et al 1987; Garbo 1990; Henderson &

Correspondence: J. E. van Lier, MRC Group in the Radiation Sciences, Faculty of Medicine, University of Sherbrooke, Sherbrooke, Québec, Canada J1H 5N4.

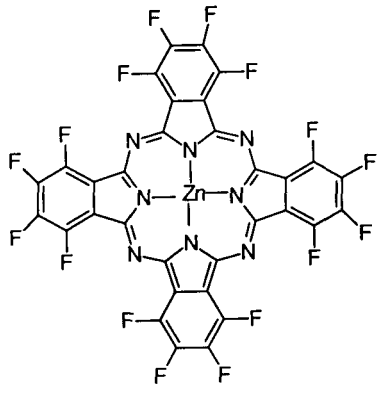

FIG. 1. Chemical structure of hexadecafluoro zinc phthalocyanine ($ZnPcF_{16}$).

Mayhew 1990). Recently, it has been demonstrated that CRM alters lipoproteins and this phenomenon has been suggested to account for the enhanced distribution to neoplastic tissues (Woodburn & Kessel 1994).

The dye chosen in this study was hexadecafluorinated zinc phthalocyanine ($ZnPcF_{16}$) (Fig. 1). It can be conveniently synthesized to yield a symmetrical, single isomeric product. This product represents the fluorinated analogue of zinc phthalocyanine (ZnPc), a compound which has recently been investigated as a possible second generation photodynamic therapy sensitizer (Ginevra et al 1990; Reddi et al 1990; Schieweck et al 1994). The fluorine atoms on $ZnPcF_{16}$ impart sufficient solubility on the molecule to allow the preparation of injectable aqueous emulsions and other colloidal drug delivery systems.

Materials and Methods

Materials

According to a previously described method, $ZnPcF_{16}$ was synthesized by condensation of tetrafluorophthalonitrile (Aldrich Chemicals Co., Milwaukee, USA) with zinc acetate dihydrate (1:1) at 160°C for 3 h (Birchall et al 1970; Boyle & van Lier 1991). The crude compound was purified by suspension in aqueous hydrogen chloride (2 M) followed by filtration, washing of the residue with ethanol and extraction into acetone. $ZnPcF_{16}$ has a molecular mass of 865. It is soluble in pyridine and in 1-methyl-2-pyrrolidinone. The main absorption peak in pyridine is at 678 nM ($\varepsilon = 2 \times 10^{-5}$). Cremophor EL was received from BASF (Toronto, Canada). PLA was a gift from Medisorb Technologies International L.P. (Cincinnati, USA) (intrinsic viscosity 0·72 dL g^{-1}). Poly(vinyl alcohol) (PVAL) was chosen as stabilizing colloid (Mowiol 4–88, Hoechst, Frankfurt, Germany). Polyethylene glycol 20000 (PEG) was used as hydrophilic coating agent for the nanoparticles. The solvents were of analytical grade and all other chemicals were commercially available.

Preparation of Cremophor emulsion

The dye was first dissolved in 1-methyl-2-pyrrolidinone, CRM (10% final) was added under sonication whereafter the solvent was discarded by means of 24 h dialysis (Spectrum dialysis bag, molecular weight cut-off 12–14 kDa, Houston, USA). 1,2-Propanediol (3% final) was then added to the solution which was diluted with phosphate-buffered saline (PBS), pH 7·4 and filtered (0·2 μM). The final concentration of $ZnPcF_{16}$ (100 μmol L^{-1}) was determined spectroscopically in pyridine.

Preparation of nanoparticles

Nanoparticles were prepared by the salting-out technique (Allémann et al 1992) and $ZnPcF_{16}$ was incorporated as follows: 25 g of an aqueous gel containing 11% of PVAL and 35% of magnesium acetate tetrahydrate was added under vigorous mechanical stirring (5500 rev min^{-1}) to an acetone solution (10 g) of 5% (w/w) PLA and 0·05% (w/w) $ZnPcF_{16}$, leading to the formation of a water-in-oil emulsion. A liquid-liquid two-phase system was actually formed due to the presence of a salting-out agent (magnesium acetate). Upon further addition of the aqueous phase, an oil-in-water emulsion was obtained. Finally, 25 g of pure water was added to allow a complete diffusion of acetone into the aqueous phase, leading to the formation of plain nanoparticles. To obtain PEG-coated nanoparticles, the last step of the preparation was modified (Leroux et al 1994). Instead of adding only 25 g pure water, 12·5 g PEG 5% was first added to the emulsion, followed by 12·5 g pure water.

The nanoparticulate suspension was purified by cross-flow filtration using a Sartocon Mini device (Sartorius, Göttingen, Germany) mounted with a polyolefin cartridge filter (100 nm pore size) (Allémann et al 1993b). After the addition of 500 mg mannitol as cryoprotective agent, the nanoparticles were freeze-dried for 24 h and stored at 4°C until use. Before administration, the nanoparticles were suspended in saline. For PEG-coated nanoparticles, sonication (10 min) was required to redisperse the particles completely.

Characterization of nanoparticles

The size of the nanoparticles was assessed by photon correlation spectroscopy (Coulter Nano-sizer, Coulter Electronics, Harpenden, Hertfordshire, UK). To determine the amount of $ZnPcF_{16}$ bound to the polymeric matrix, 5 mg of nanoparticles was dissolved in pyridine, the solution was sonicated for 15 min and assayed spectrophotometrically at 678 nM (Hitachi spectrophotometer, U-2000, Tokyo, Japan). The PEG content in nanoparticles can be assessed by colorimetry (Leroux et al 1994). PEG in acidic solutions forms a complex with iodine in the presence of barium chloride (Childs 1975). Nanoparticles (20 mg) were mixed with 5 mL chloroform to dissolve the PLA and the PEG. The solution was sonicated for 30 min. A 1-mL aliquot was sampled and mixed with 10 mL water. The chloroform was then evaporated under reduced pressure to allow precipitation of PLA and diffusion of PEG in water. Water lost during evaporation was replaced. An aliquot of the PEG aqueous solution was added to 3 mL water, 1 mL barium chloride solution (5% in 1 M HCl) and 0·5 mL 1·27% iodine –2·5% potassium iodide in water. The absorbance (505 nm) was recorded immediately after the addition of iodine.

Animal experiments

All experiments were performed on male BALB/c mice (19–23 g) (Charles River Breeding Laboratories, Montreal, Canada). These experiments were conducted following a protocol approved by the Canadian Council on Animal Care and an in-house ethics committee. The animals were allowed free access to water and food throughout the course

of the experiments. EMT-6 mouse mammary tumour cells were maintained according to an established protocol (Rockwell et al 1972), as previously described (Brasseur et al 1993). Before tumour implantation, hair on the hind legs and back of the mice was removed by shaving and chemical depilation (Nair, Whitehall, Mississauga, Canada). A tumour was implanted on each hind thigh by intradermal injection of 2×10^5 EMT-6 cells suspended in 0·05 mL Waymouth growth medium (Gibco, Canada). Mice were used 10 or 11 days after cell inoculation when the tumour diameter and thickness reached 4–8 mm and 2–4 mm, respectively.

Biodistribution

Tumour-bearing mice were injected intravenously via the caudal vein with 1 μmol kg^{-1} of $ZnPcF_{16}$ formulated either in CRM, in plain PLA nanoparticles or in PEG-coated nanoparticles (0·2 mL). At different time intervals after dye administration (3, 6, 12, 24, 48, 72 and 168 h), blood was collected from the axillary vessels in the angle of the forelimb by means of heparinized syringes, whereafter the animals (n = 5) were killed. Organs and tissues of interest were then removed, washed with saline (0·9% NaCl) and blotted dry.

One millilitre of water was added to blood samples (100 mg) to induce haemolysis. The samples were then frozen (−40°C) and subsequently freeze-dried over 48 h to eliminate water completely. After this step 3·0 mL *N,N*-dimethylformamide (DMF) was added to the lyophilisates. Homogenization was achieved by sonication. Homogenates were incubated overnight at 37°C under mechanical agitation and then centrifuged at 2800 *g* for 20 min. The supernatants were sampled and further centrifuged under the same conditions. The dye concentration in the clear supernatant was assayed by fluorescence (Fluorescence spectrophotometer F-2000, Hitachi, Tokyo, Japan) (λ_{ex} 766 nm, λ_{em} 780 nm, 5 nm band pass). Whole tumours (40–80 mg) and aliquots of other organs (80–150 mg) were homogenized with 2·0 mL DMF using a Polytron fitted with a PT 10/35 rotor (Brinkman, Rexdale, Ontario, Canada). Then, the samples were incubated and centrifuged as for blood samples.

Fluorescence intensity of $ZnPcF_{16}$ extracted from tissue samples in DMF varied as a function of water content. An increase in water content, due to a heavier tissue sample, decreased the fluorescence intensity. This is because of aggregation of $ZnPcF_{16}$ when the solvent mixture becomes more polar. To correct fluorescence intensity for the percentage of water in the samples, calibration curves of dye dissolved in DMF containing variable amounts of water were used. Following this intensity correction, calibration curves for the different organs were used to determine the concentration of dye in the samples. Calibration curves were established by adding known amounts of dye to 80–150 mg to tissue from control mice, whereafter the tissues were treated as described above. No fluorescence was found in control tissue samples to which no dye had been added.

Results

Preparation and characterization of nanoparticles

Uncoated nanoparticles had a mean size of 464 nm and a drug load of 0·66%. PEG-coated nanoparticles had a mean size of 988 nm and a drug load of 0·61%. The addition of PEG during the dilution step of the preparation procedure increased the mean size of the particles (Leroux et al 1994). In this study, it was not possible to reduce the size of the PEG-coated particles by increasing the PLA concentration in the organic phase of the emulsion because of the low solubility of the compound in the organic phase (Allémann et al 1992). This would have reduced the initial dye/polymer ratio resulting in a lower undesired drug loading. The PEG content of the coated particles represented 2% (w/w) of the nanoparticles.

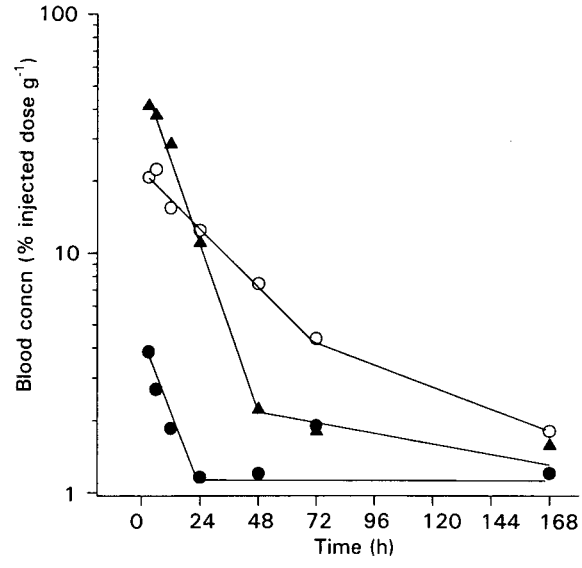

FIG. 2. Blood concentration (% injected dose g^{-1}) of $ZnPcF_{16}$ in EMT-6 tumour-bearing mice after intravenous injection of dye (1 μmol kg^{-1}; 0·865 mg kg^{-1}) formulated in PLA nanoparticles (●), PEG-coated PLA nanoparticles (○), and CRM emulsion (▲) (n = 5).

Due to the necessity of using PVAL as stabilizing colloid during the emulsification, purified nanoparticles contain residues of this polymer, which is probably distributed on the nanoparticles surface. PVAL content is related to the particles' specific surface area (Allémann et al 1993c). In this study, 464-nm particles contain approximately 3% (w/w) of PVAL and particles of 988 nm less than 1% (w/w).

Biodistribution of $ZnPcF_{16}$ incorporated in nanoparticles

The two types of nanoparticles investigated in this study gave rise to significantly different distributions of $ZnPcF_{16}$ in organs. These differences are obvious, when comparing the blood clearances (Fig. 2). Like most types of nanoparticles, plain PLA nanoparticles were cleared very rapidly from the blood circulation. After 3 h the concentration of dye in blood was only 0·83 μg g^{-1}. Although very low at this time, the concentration continued to decrease with a short half-life ($t_{\frac{1}{2}}$ = 10 h) until 24 h. The resulting bioavailability of $ZnPcF_{16}$ was very low (AUC_{0-168} = 57 μg h g^{-1}), the area under the blood concentration–time curve being calculated by the trapezoidal rule. Important concentrations of $ZnPcF_{16}$ administered in plain nanoparticles were found in the liver, spleen and lungs (Table 1). The combined accumulation of the dye in these three organs represented up to 64% of the injected dose at 24 h post-injection (Table 2). From 24 h to 7 days the total amount of drug in these organs decreased to 47% of the injected dose. Probably due to a

Table 1. Tissue concentration (s.e.m.) of $ZnPcF_{16}$ (1 $\mu g\,g^{-1}$ = 5% injected dose g^{-1}) in EMT-6 tumour-bearing mice after intravenous injection of dye (1 $\mu mol\,kg^{-1}$; 0·865 mg kg^{-1}) formulated in different vehicles (n = 5).

Tissue	Concentration ($\mu g\,g^{-1}$)						
	3 h	6 h	12 h	24 h	48 h	72 h	168 h
PLA nanoparticles							
Blood	0·83	0·58	0·40	0·25	0·26	0·41	0·26
	(0·05)	(0·02)	(0·02)	(0·01)	(0·02)	(0·02)	(0·02)
Plasma	1·01	0·66	0·83	0·83	0·65	0·43	0·589
	(0·09)	(0·10)	(0·24)	(0·24)	(0·05)	(0·06)	(0·10)
Tumour	1·88	1·71	1·16	1·20	1·57	1·25	1·04
	(0·40)	(0·29)	(0·14)	(0·04)	(0·22)	(0·17)	(0·29)
Muscle	b.d.l.	0·27	0·10	0·41	0·12	0·33	b.d.l.
		(0·15)	(0·07)	(0·09)	(0·06)	(0·06)	
Skin	0·41	0·70	0·57	0·38	0·21	0·20	b.d.l.
	(0·11)	(0·17)	(0·16)	(0·09)	(0·06)	(0·06)	
Liver	7·58	9·40	8·95	9·36	7·20	7·67	6·63
	(1·05)	(0·86)	(0·57)	(1·28)	(0·58)	(0·26)	(0·59)
Spleen	30·94	26·40	29·59	29·82	27·65	25·25	22·48
	(3·43)	(2·43)	(1·61)	(2·05)	(1·08)	(1·52)	(0·76)
Lung	5·33	4·57	3·69	2·55	1·75	1·51	2·15
	(0·74)	(0·43)	(0·32)	(0·19)	(0·17)	(0·20)	(0·35)
Kidney	0·56	0·41	0·33	0·25	0·22	0·23	0·20
	(0·04)	(0·05)	(0·03)	(0·03)	(0·03)	(0·02)	(0·01)
PEG-coated PLA nanoparticles							
Blood	4·45	4·82	3·32	2·68	1·60	0·94	0·39
	(0·26)	(0·11)	(0·12)	(0·09)	(0·05)	(0·04)	(0·02)
Plasma	5·81	5·82	4·07	3·08	1·57	1·05	0·61
	(0·35)	(0·23)	(0·32)	(0·26)	(0·05)	(0·08)	(0·07)
Tumour	2·25	2·62	3·17	2·78	4·01	3·00	1·55
	(0·05)	(0·12)	(0·35)	(0·21)	(0·48)	(0·34)	(0·10)
Muscle	b.d.l.	b.d.l.	0·35	0·18	0·37	0·27	b.d.l.
			(0·10)	(0·04)	(0·13)	(0·06)	
Skin	0·70	0·55	0·87	1·02	1·14	1·04	0·81
	(0·08)	(0·06)	(0·08)	(0·07)	(0·11)	(0·10)	(0·17)
Liver	5·77	6·69	5·66	6·97	5·60	6·31	4·94
	(0·52)	(0·27)	(0·60)	(0·18)	(0·55)	(0·30)	(0·33)
Spleen	36·24	33·21	37·90	31·36	27·64	19·39	10·15
	(2·59)	(3·68)	(2·71)	(2·73)	(2·20)	(1·97)	(0·77)
Lung	7·09	6·31	5·04	4·18	3·28	2·97	2·30
	(0·51)	(0·26)	(0·40)	(0·16)	(0·37)	(0·24)	(0·40)
Kidney	1·06	1·00	0·96	0·93	0·79	0·67	0·50
	(0·12)	(0·08)	(0·08)	(0·02)	(0·03)	(0·05)	(0·04)
CRM emulsion							
Blood	8·90	8·12	6·13	2·38	0·48	0·39	0·34
	(0·15)	(0·44)	(0·35)	(0·13)	(0·04)	(0·02)	(0·04)
Plasma	13·19	12·38	8·99	3·13	1·27	0·92	0·94
	(0·70)	(0·95)	(0·37)	(0·21)	(0·30)	(0·09)	(0·11)
Tumour	2·61	2·93	3·48	3·63	3·33	2·60	2·04
	(0·20)	(0·12)	(0·36)	(0·33)	(0·26)	(0·10)	(0·15)
Muscle	0·65	0·41	0·45	0·51	0·32	0·33	0·10
	(0·07)	(0·10)	(0·07)	(0·08)	(0·09)	(0·05)	(0·04)
Skin	1·53	1·48	2·34	1·48	1·38	1·50	1·02
	(0·13)	(0·12)	(0·29)	(0·09)	(0·23)	(0·08)	(0·20)
Liver	2·02	2·35	5·17	8·45	9·47	10·18	10·46
	(0·28)	(0·22)	(0·27)	(0·51)	(0·86)	(0·89)	(0·56)
Spleen	2·01	2·66	3·34	5·33	6·02	6·36	5·76
	(0·24)	(0·21)	(0·48)	(0·36)	(0·44)	(0·59)	(0·27)
Lung	2·51	2·72	1·40	0·76	0·62	0·54	0·47
	(0·11)	(0·45)	(0·17)	(0·13)	(0·03)	(0·02)	(0·07)
Kidney	0·86	1·06	0·81	0·43	0·35	0·25	0·27
	(0·04)	(0·07)	(0·02)	(0·02)	(0·02)	(0·01)	(0·03)

very rapid blood clearance, tumour concentrations remained low with this formulation (1·2–1·9 $\mu g\ g^{-1}$). $ZnPcF_{16}$ loaded in PEG-coated nanoparticles exhibited a totally different blood clearance (Fig. 2), reflecting an extended circulation of the dye. During the time course of the experiment, blood clearance followed first-order kinetics with a $t_{\frac{1}{2}}$ of about 30 h. A fourfold increase in AUC was observed when compared with the plain nanoparticles ($AUC_{0-168} = 227\ \mu g\ h\ g^{-1}$). The concentration of the dye in the liver was lower than with plain nanoparticles (Table 1). Although spleen dye levels were slightly higher shortly after injection, they decreased faster than with the plain nanoparticle formulation. Due to their larger size, PEG-coated nanoparticles were partially filtered by the lungs. However, this was a transient phenomenon. Combined accumulation of $ZnPcF_{16}$ in the three main reservoir organs was 56% of the injected dose at the beginning of the experiment and decreased to as low as 33% at the end of the experiment (Table 2). With this formulation, the tumour accumulated significant amounts of photosensitizer, reaching a maximum of 4·01 $\mu g\ g^{-1}$ (22% injected dose g^{-1}) at 48 h post-injection.

Table 2. Cumulated percentage of injected dose in the liver, spleen and lungs of EMT-6 tumour-bearing mice after intravenous injection of 1 μmol kg^{-1} $ZnPcF_6$ incorporated in different vehicles (n = 5).

Tissue	Cumulative dose (%)						
	3 h	6 h	12 h	24 h	48 h	72 h	168 h
PLA nanoparticles							
Liver	37·13	46·09	43·85	45·86	35·29	37·61	32·51
Spleen	15·55	13·27	14·87	14·99	13·90	12·69	11·30
Lung	7·32	6·28	5·07	3·50	2·40	2·08	2·95
PEG-coated PLA nanoparticles							
Liver	28·29	32·81	27·73	34·17	27·46	30·95	24·23
Spleen	18·22	16·70	19·05	15·77	13·90	9·75	5·10
Lung	9·74	8·67	6·94	5·74	4·51	4·08	3·16
CRM emulsion							
Liver	9·90	11·53	25·36	41·41	46·40	49·88	51·26
Spleen	1·00	1·33	1·68	2·67	3·02	3·19	2·89
Lung	3·45	3·73	1·92	1·04	0·84	0·74	0·64

Biodistribution of $ZnPcF_{16}$ incorporated in CRM

The CRM oil-in-water emulsion did not allow high blood levels of the dye over an extended period of time ($t_{\frac{1}{2}}$ = 12 h). However, since there was no early uptake by the liver and spleen (Table 1) blood levels were higher than with the PEG-coated nanoparticles up to 24 h. The relative bioavailability was comparable to that observed with coated nanoparticles (AUC_{0-168} = 213 μg h g^{-1}). Contrary to the findings with both nanoparticulate formulations, concentrations in the liver and spleen increased over the time course of the experiment (Table 2) leading to a final accumulation of 55% of the injected dose of $ZnPcF_{16}$ in the three main reservoirs. With this formulation, a significant accumulation of the dye in the tumour was observed, reaching a maximum of 3·63 μg g^{-1} (20% g^{-1}) 24 h post-injection.

Tumour to organ ratios

The two most promising formulations for the delivery of $ZnPcF_{16}$ to EMT-6 mammary tumours (PEG-coated nanoparticles and CRM emulsion) were compared in detail. Tumour-to-skin and tumour-to-muscle uptake ratios were calculated. These parameters are important to predict the risk of damage to tumour-adjacent tissues during the photodynamic therapy. Both CRM and PEG-coated nanoparticle formulation gave rise to advantageous tumour-to-skin ratios (Table 3), although the ratio for CRM was slightly lower throughout the whole experiment. Tumour-to-muscle ratios were very high for both formulations, with values around 10 at 48 h post-injection. The tumour-to-blood ratios remained low up to 24 h for both formulations, but from 48 h post-injection, favourable ratios were observed. At this time point, the CRM formulation exhibited the highest dye uptake ratios due to rapid blood clearance.

Table 3. Tumour-uptake ratios of $ZnPcF_{16}$ incorporated in PEG-coated PLA nanoparticles and CRM EL emulsion after intravenous injection of 1 μmol kg^{-1} (n = 5).

Tissue	Ratio						
	3 h	6 h	12 h	24 h	48 h	72 h	168 h
PEG-coated PLA nanoparticles							
Tumour/skin	3·23	4·73	3·65	2·72	3·5	2·89	1·91
Tumour/muscle			8·97	15·05	10·75	11·03	
Tumour/blood	0·51	0·54	0·95	1·04	2·51	3·18	3·93
CRM EL emulsion							
Tumour/skin	1·7	1·98	1·49	2·45	2·41	1·73	1·99
Tumour/muscle	4·02	7·09	7·73	7·18	10·35	7·94	21·06
Tumour/blood	0·29	0·36	0·57	1·52	6·94	6·64	5·99

Discussion

In a previous in-vitro study (Leroux et al 1994), it was demonstrated that drug delivery via PEG-coated PLA nanoparticles as compared with plain nanoparticles could significantly reduce the uptake by monocytes. In the present study we have confirmed that PEG-coating of nanoparticles by the salting-out procedure, reduces liver uptake, and therefore enhances significantly (fourfold) the relative bioavailability of the drug. The protection of colloidal particles against phagocytic cells has been attributed to the formation of a hydrophilic uncharged coating (Müller & Wallis 1993). Hydrophilicity alone, however, is not a sufficient condition to reduce the RES uptake. As a matter of fact, PVAL-coated nanoparticles are cleared very rapidly from the bloodstream. By modifying the salting-out procedure with the addition of PEG during the dilution step, the surface properties of the particles are modified such as to change their binding properties (Leroux et al 1994).

Spleen uptake of the dye with the PEG-coated nanoparticles was only transiently higher, and decreased faster than with plain nanoparticles. As stated elsewhere, this uptake could be significantly reduced if the coated nanoparticles were smaller (Davis et al 1993). Lung levels were higher, which is probably due to capillary filtration of the coated particles which have a larger size than plain nanoparticles. With PEG-coated nanoparticles significant amounts of dye accumulated in the tumour reaching a maximum concentration at 48 h post-injection and remaining high throughout the experiment. Low dye concentrations in the muscle and skin provided favourable tumour-to-muscle ratios (ranging from 9 to 15) and tumour-to-skin ratios (ranging from 2·7 to 4·7). At these ratios, damage to healthy tissues surrounding the tumour will be minimal during phototherapy.

$ZnPcF_{16}$ formulated in CRM also exhibited a high relative bioavailability. The high blood levels observed up to 24 h led to the accumulation of dye in the tumour, reaching earlier maximum concentrations as compared with the coated particles. Although slightly lower than with PEG-coated nanoparticles, tumour-to-muscle and tumour-to-skin ratios also were favourable. These ratios remained stable from 24 to 72 h. However, the tumour-to-blood ratio increased significantly during the same period of time, reflecting rapid blood clearance. Tumour to blood ratios at the time of photodynamic therapy are important with regard to the type of mechanism by which the photodynamic action induces tumour regression. High tumour-to-blood ratios should favour a direct tumour cell death, whereas tumour necrosis in conjunction with low ratios is indicative of an indirect cell kill mechanism, involving anoxia in the tumour tissue following microvasculature occlusion (Zhou 1989). Contrary to nanoparticle formulations, the total amount of dye in the liver, spleen and lungs increased continuously during the experiment, reaching 55% at 7 days post-injection. This observation is important with regard to possible toxicity. Indeed, it should be noted that clinical use of CRM has

been associated with anaphylactoid reactions (Dye & Watkins 1980), hyperlipidaemia and abnormal electrophoretic lipoprotein patterns (Bagnarello et al 1977).

In conclusion, PEG-coated nanoparticles are promising formulations with regard to their ability to deliver $ZnPcF_{16}$ to EMT-6 mammary mouse tumours. Both CRM and PEG-coated nanoparticles are clearly superior dye vehicles as compared with plain nanoparticles. Considering tumour uptake and tumour-to-organ ratios, the best protocol for in-vivo photodynamic therapy in this animal model would be 48 h post-injection, in the case of the PEG-coated nanoparticles. For the CRM emulsion, this time point likewise appears as the most appropriate, even though at 24 h, tumour dye concentrations are somewhat higher. The substantially lower blood concentration at 48 h vs 24 h post-injection results in maximum tumour-to-blood ratios at 48 h which should provide more advantageous conditions for direct cell kill. Such considerations warrant comparative photodynamic therapy assays with these formulations at both 24 h and 48 h post-injection.

Acknowledgements

The authors are grateful to the Medical Research Council of Canada for generous financial support of this work. E. Allémann acknowledges a fellowship from the Swiss National Science Foundation and J.-C. Leroux acknowledges a fellowship from the Medical Research Council of Canada.

References

Allémann, E., Gurny, R., Doelker, E. (1992) Preparation of aqueous polymeric nanodispersions by a reversible salting-out process, influence of process parameters on particle size. Int. J. Pharm. 87: 247–253

Allémann, E., Gurny, R., Doelker, E. (1993a) Drug loaded nanoparticles—preparation methods and drug targeting issues. Eur. J. Pharm. Biopharm. 39: 173–191

Allémann, E., Doelker, E., Gurny, R. (1993b) Drug loaded poly(lactic acid) nanoparticles produced by a reversible salting-out process: purification of an injectable dosage form. Eur. J. Pharm. Biopharm. 39: 13–18

Allémann, E., Leroux, J. C., Gurny, R., Doelker, E. (1993c) In vitro sustained release properties of drug loaded poly(D,L-lactic acid) nanoparticles produced by a salting-out procedure. Pharm. Res. 10: 1732–1737

Bagnarello, A. G., Lewis, L. A., McHenry, M. C., Weinstein, A. J., Naito, H. K., McCullough, A. J., Lederman, R. J., Gavan, T. L. (1977) Unusual serum lipoprotein abnormality induced by the vehicle of miconazole. N. Engl. J. Med. 296: 497–499

Birchall, J. M., Haszeldine, R. N., Morley, J. O. (1970) Polyfluoroarenes. Part XIV. Synthesis of halogenophthalocyanines. J. Chem. Soc. (C) 9: 2667–2672

Boyle, R. W., van Lier, J. E. (1991) Fluorophthalocyanines as photosensitizers for cancer therapy. Eur. Soc. Photobiol. Conf. Proc., Abstract A19, p. 58

Brasseur, N., Brault, D., Couvreur, P. (1991) Adsorption of hematoporphyrin onto polyalkylcyanoacrylate nanoparticles: carrier capacity and drug release. Int. J. Pharm. 70: 129–135

Brasseur, N., Nguyen, T. L., Langlois, R., Ouellet, R., Marengo, S., Houde, D., van Lier, J. E. (1993) Synthesis and photodynamic activities of silicon 2,3-naphthalocyanine derivatives. J. Med. Chem. 37: 415–420

Childs, C. E. (1975) The determination of polyethylene glycol in gamma globulin solutions. Microchem. J. 20: 190–192

Davis, S. S., Illum, L., Moghimi, S. M., Davies, M. C., Porter, C. J. H., Muir, I. S., Brindley, A., Christy, N. M., Norman, M. E., Williams, P., Dunn, S. E. (1993) Microspheres for targeting drugs to specific body sites. J. Contr. Rel. 24: 157–163

Dunn, S. E., Brindley, A., Davies, M. C., Davis, S. S., Illum, L. (1992) Studies on in-vitro uptake by Kupffer cells and the in-vivo biodistribution of a range of novel polymeric colloids. J. Pharm. Pharmacol. 44: 1082

Dye, D., Watkins, J. (1980) Suspected anaphylactic reaction to Cremophor EL. Br. Med. J. 280: 1353

Garbo, G. M. (1990) The use of liposomes, emulsions or inclusion complexes may potentiate in vivo effects of SnET2. Proc. Int. Soc. Optical Eng. 1203: 118–125

Ginevra, F., Biffanti, S., Pagnan, A., Biolo, R., Reddi, E., Jori, G. (1990) Delivery of the tumour photosensitizer zinc(II)-phthalocyanine to serum proteins by different liposomes: studies in vitro and in vivo. Cancer Lett. 49: 59–65

Henderson, B. W., Dougherty, T. J. (1992) How does photodynamic therapy work? Photochem. Photobiol. 55: 145–157

Henderson, B. W., Mayhew, E. (1990) Experience with the liposomal delivery of the photosensitizer isoBoSiNc. Proc. Int. Soc. Optical Eng. 1203: 126–135

Illum, L., Davis, S. S. (1987) Targeting of colloidal particles to the bone marrow. Life Sci. 40: 1553–1560

Illum, L., Davis, S. S., Müller, R. H., Mak, E., West, P. (1987) The organ distribution and circulation time of intravenously injected colloidal carriers sterically stabilized with a block copolymer-poloxamine 908. Life Sci. 40: 367–374

Jori, G., Tomio, L., Reddi, E., Rossi, E., Corti, L., Zorat, P. L., Calzavara, F. (1983) Preferential delivery of liposome-incorporated porphyrins to neoplastic cells in tumour-bearing rats. Br. J. Cancer 48: 307–309

Labib, A., Lenaerts, V., Chouinard, F., Leroux, J. C., Ouellet, R., van Lier, J. E. (1991) Biodegradable nanospheres containing phthalocyanines and naphthalocyanines for targeted photodynamic tumor therapy. Pharm. Res. 8: 1027–1031

Leroux, J. C., Gravel, P., Balant, L., Volet, B., Anner, B. M., Allémann, E., Doelker, E., Gurny, R. (1994) Internalization of poly(d,l-lactic acid) nanoparticles by isolated human leukocytes and analysis of plasma proteins adsorbed onto the particles. J. Biomed. Mater. Res. 28: 471–481

Müller, R. H., Wallis, K. H. (1993) Surface modification of i.v. injectable biodegradable nanoparticles with poloxamer polymers and poloxamine 908. Int. J. Pharm. 89: 25–31

Reddi, E., Zhou, C., Biolo, R., Menegaldo, E., Jori, G. (1990) Liposome- or LDL-administered Zn(II)-phthalocyanine as a photodynamic agent for tumours. I. Pharmacokinetic properties and phototherapeutic efficiency. Br. J. Cancer 61: 407–411

Rockwell, S. C., Kallman, R. F., Fajardo, L. F. (1972) Characteristics of serially transplanted mouse mammary tumor and its tissue-culture-adapted derivative. J. Natl. Cancer Inst. 49: 735–749

Rosenthal, I. (1991) Phthalocyanines as photodynamic sensitizers. Photochem. Photobiol. 53: 859–870

Selman, S. H., Garbo, G. M., Keck, R. W., Kreimer-Birnbaum, M., Morgan, A. R. (1987) A dose response analysis of purpurin derivatives used as photosensitizers for the photodynamic treatment of transplantable FANFT induced urothelial tumors. J. Urol. 137: 1255–1257

Schieweck, K., Capraro, H.-G., Isele, U., van Hoogevest, P., Ochsner, M., Maurer, T., Batt, E. (1994) CGP 55 847, liposome-delivered zinc(II)-phthalocyanine as a phototherapeutic agent for tumors. Proc. Int. Soc. Optical Eng. 2078: 107–118

Tan, J. S., Butterfield, D. E., Voycheck, C. L., Caldwell, K. D., Li, J. T. (1993) Surface modification of nanoparticles by PEO/PPO block copolymers to minimize interactions with blood components and prolong blood circulation in rats. Biomaterials 14: 823–833

Tröster, S. D., Kreuter, J. (1992) Influence of the surface properties of low contact angle surfactants on the body distribution of ^{14}C-poly(methyl methacrylate) nanoparticles. J. Microencaps. 9: 19–28

Tröster, S. D., Müller, U., Kreuter, J. (1990) Modification of the body distribution of poly(methyl methacrylate) nanoparticles in rats by coating surfactants. Int. J. Pharm. 61: 85–100

van Lier, J. E. (1990) Phthalocyanines as sensitizers for the photodynamic therapy of cancer. In: Kessel, D. (ed.) Photodynamic Therapy of Cancers. Vol. I, CRC Press, Boca Raton, pp. 279–291

Woodburn, K., Kessel, D. (1994) The alteration of plasma lipoproteins by Cremophor EL. J. Photochem. Photobiol. B: Biol. 22: 197–201

Zhou, C. N. (1989) Mechanisms of tumor necrosis induced by photodynamic therapy. J. Photochem. Photobiol. B: Biol. 3: 299–318